https://doi.org/10.5194/mr-2021-65
Preprint. Discussion started: 6 December 2021

Open Access MAGNETIC RESONANCE Discussions

Radiation damping strongly perturbs remote resonances in presence of homo-nuclear mixing sequences

Philippe Pelupessy[1]

[1]Laboratoire des Biomolécules, LBM, Département de Chimie, École Normale Supérieure, PSL University, Sorbonne Université, CNRS, 75005 Paris, France

Correspondence: Philippe Pelupessy (philippe.pelupessy@ens.psl.eu)

Abstract. In this work, it is experimentally shown that the weak oscillating magnetic field (known as the "radiation damping" field) caused by the inductive coupling between the transverse magnetization of nuclei and the radio frequency circuit perturbs remote resonances when homo-nuclear total correlation mixing sequences are applied. Numerical simulations are used to rationalize this effect.

1 Introduction

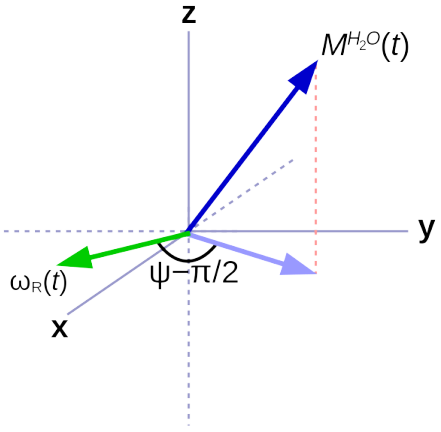

Figure 1. The RD field lies in the xy-plane. It has an amplitude that is proportional to the projection of the water magnetization onto the same plane and a phase of $\psi - \pi/2$ with respect to this projection.

The coupling between precessing magnetization and a radio-frequency (RF) circuit induces an RF field, which in turn affects the evolution of the magnetization and hence the appearance of NMR spectra. The existence of this phenomenon was first hypothesized by Suryan (Suryan (1949)), while a more rigorous theoretical description was later provided by Bloembergen and Pound (Bloembergen and Pound (1954)). The latter introduced the term radiation damping (RD), an expression which, as several authors have stated before (Abragam (1961); Vlassenbroek et al. (1995); Hoult and Bhakar (1997); Krishnan and Murali

https://doi.org/10.5194/mr-2021-65
Preprint. Discussion started: 6 December 2021


Open Access MAGNETIC RESONANCE Discussions

(2013)), is rather misleading with both radiation and damping called into question. The expression "Radiation feedback" has been suggested as an alternative, however this term is often used to designate active feedback circuits to enhance (Szoke and Meiboom (1959); Hobson and Kaiser (1975)) or eliminate (Louisjoseph et al. (1995); Broekaert and Jeener (1995)) the effects of radiation damping. Another option, in analogy with quantum backaction, could be *induction backaction*. In order to avoid confusion, the term RD will nevertheless be employed in this work. When no other RF fields are present, the RD field rotates the magnetization that is responsible for the induced RF field towards its equilibrium direction (Bloom (1957)), parallel to the main field, leaving the norm unchanged (if it is homogeneous in space, as with any RF field). In liquid state NMR, this effect is usually weak and only noticeable when the magnetization is strong, either for nuclei in molar concentrations (such as for partially- or non-deuterated solvents) or when the polarization is enhanced.

The RD field strongly affects the resonances with frequencies close to the one that is at its origin and remote resonances that are directly coupled by scalar or dipolar interactions (Miao et al. (1999)) or undergo chemical exchange (Chen and Mao (1997)) with the nuclei that induce RD. Subtle effects on remote resonances (Sobol et al. (1998)) can affect sensitive difference experiments. Homo-nuclear isotropic mixing sequences which have been designed for total correlation spectroscopy (TOCSY), however, are very efficient at removing the chemical shift differences from the effective Hamiltonian (Braunschweiler and Ernst (1983); Bax and Davis (1985)). In this work, it will be shown that RD, in presence of suitable mixing sequences, can heavily perturb spins over wide range of resonance frequencies.

2 Materials and Methods

All experiments have been performed on a Bruker NMR spectrometer in a field of 14.1 T (600 MHz proton frequency) equipped with a probe cooled by liquid nitrogen ("Prodigy") with coils to generate pulsed field gradients along the z-axis. This study has been done on a standard calibration sample that contained, among other substances, about 80% H_2O and 20% HDO ($i.e.$, close to 100 M solvent protons) and 0.5 mM Sodium-trimethyl-silyl-propane-sulfonate (DSS). At the experimental temperature of 298 K, the chemical shift difference between the solvent and the methyl protons is $ca.$ 4.78 ppm (2868 Hz at 14.1 T, the water resonance being "downfield", i.e., precessing at a higher negative frequency).

The selective TOCSY experiment (Davis and Bax (1985); Kessler et al. (1986)) used in this work, with an optional bipolar gradient pair for coherence pathway selection (Dalvit and Bovermann (1995)), is described in figure 2. A selective pulse applied to the solvent A, followed by a pulsed field gradient, can be inserted before the sequence so that the magnitude of the longitudinal magnetization M_z^A can be controlled and hence the strength of the RD effect. If, instead of the transverse magnetization, one wishes to monitor the z-component of the magnetization that remains after the homo-nuclear mixing sequence, a gradient followed by a $\pi/2$ pulse can be inserted just before acquisition. For homonuclear transfer, an isotropic mixing pulse train, DIPSI-2 (Rucker and Shaka (1989)), has been chosen with an RF amplitude $\gamma B_1/2\pi = 4.17$ kHz (which corresponds to a duration of 60 μs for a $\pi/2$ pulse). Selective excitation, either on the water or on the methyl protons, has been achieved with a Gaussian $\pi/2$ pulse of 5 ms.

https://doi.org/10.5194/mr-2021-65
Preprint. Discussion started: 6 December 2021

Open Access MAGNETIC RESONANCE Discussions

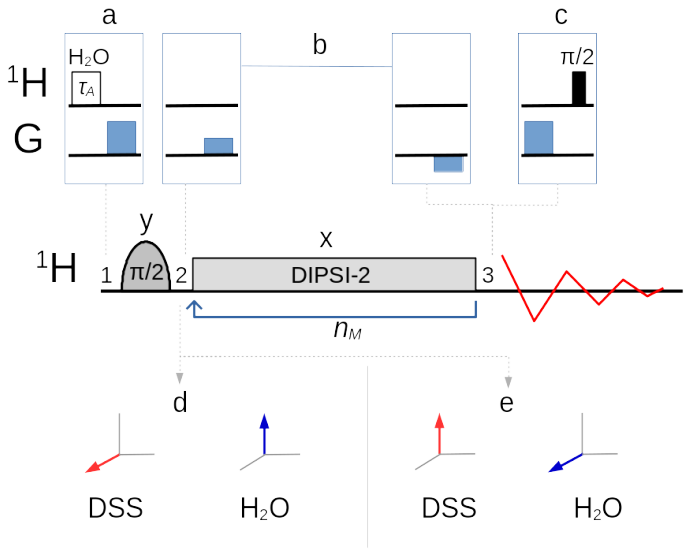

Figure 2. Selective TOCSY sequence. The magnetization of one nuclear spin species is rotated into the transverse plane by the selective $\pi/2$ pulse, followed by a DIPSI-2 pulse train which is repeated n_M times. Neglecting relaxation and coherence transfer, the isotropic mixing DIPSI-2 sequence is designed to leave the magnetization unchanged (spin-locked) across a wide band of frequencies centered on the RF carrier frequency. The selective pulse is cycled through $(y, -y, -y, y)$ with a concomitant alternation of the receiver phase. (a) A selective pulse of duration τ_A applied to the water resonance followed by a pulsed field gradient can be inserted at position 1 to tune the amplitude of the longitudinal components of the water magnetization between $+M^{eq}$ and $-M^{eq}$. (c) At position 3, a pulsed field gradient followed by a $\pi/2$ pulse permits the detection of M_z. (b) An optional bipolar pulsed field gradient pair at positions 2 and 3 on either side of the mixing interval leads to a cleaner coherence pathway selection and a higher signal-to-noise ratio if the receiver gain can be increased, albeit at the cost of some signal decay due to translational diffusion. In this work the carrier frequency was set either on the three methyl group resonances of DSS (leading to the situation -immediately after the selective $\pi/2$ pulse- shown in d) or on the water resonance (e).

The programs for numerical simulations of the trajectories of the magnetization and to extract the experimental peak intensities were written in the Python language. In particular, the evolution of the magnetization under the TOCSY pulse train (governed by the set of non-linear coupled differential equations 1-3) was numerically evaluated with the SciPy integration libraries (Virtanen et al. (2020)) using an explicit Runge-Kutta method of order 5 (RK5(4)) (Shampine (1986)).

3 Experimental Results

The selective TOCSY experiment of figure 2 was applied with the RF carrier frequency set on the protons of the three methyl groups of DSS. The isotropic mixing module, DIPSI-2, consists of 36 RF pulses of constant amplitude and varying duration, applied along $+x$ or $-x$ and is repeated n_M times (Rucker and Shaka (1989)). Since the excited methyl spins S are not coupled, the mixing sequence acts as a spin-lock and only a relaxation-induced decay should be observed as n_M increases.

https://doi.org/10.5194/mr-2021-65
Preprint. Discussion started: 6 December 2021

Open Access MAGNETIC RESONANCE Discussions

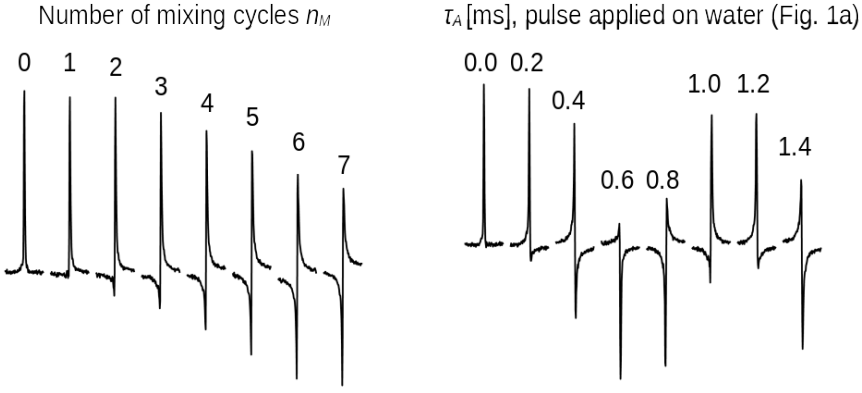

Figure 3. Spectra of the protons of the three methyl groups of DSS obtained with the experiment of figure 2 with the carrier set at the methyl resonance frequency (conditions before mixing as in figure 2d). The selective $\pi/2$ pulse had a Gaussian profile of 5 ms. The strength of the RF amplitude during mixing was 4.2 kHz. (left) As the number of cycles n_M increases, the signal changes phase. Each pulse train cycle takes about 7 ms to complete. After 26 cycles the resonance is back close to its initial phase (corresponding to a precession frequency close to 5.5 Hz). (right) The amount of z-magnetization of H_2O is varied by applying a rectangular pulse with 250 Hz amplitude and a length τ_A (marked on top of each spectrum) to the water resonance followed by a pulsed field gradient (figure 2a) immediately before the sequence with $n_M = 26$. All spectra have the same phase corrections.

Nevertheless, the spectra of figure 3 (left) show a clear phase-drift, making nearly a full turn at $n_M = 26$. The change of phase depends strongly on the water M_z^A magnetization at the beginning of the experiment, as can be seen on the right of the figure: for $n_M = 26$, immediately before the selective TOCSY sequence, an RF pulse applied to the H_2O resonance of varying length τ_A, followed by a gradient, has been inserted, so as to modify at will M_z^A before the isotropic mixing sequence.

In figure 4 (left), the phase variations of the latter experiment are plotted as a function of τ_A. The theoretical curve in orange predicts the phase evolution if the phase is proportional to the initial water longitudinal magnetization, M_z^A, and the RF pulse on the water is ideal (i.e., with a nutation angle equal to $\omega_1\tau_A$). The deviations between the curve and the experimental points are due to RF inhomogeneities, RD during the pulse applied to water, slight miss-calibrations of the RF power and a possible small miss-estimation of the initial phase-shift. At positions a ($\tau_A = 0$ ms, when the water magnetization is unperturbed), b ($\tau_A = 1.1$ ms, when the water magnetization approximately vanishes) and c ($\tau_A = 2.2$ ms, when the water magnetization is approximately inverted) the phase evolution has been recorded as a function of number n_M of isotropic mixing cycles, as shown in figure 4 (right). The dashed curve corresponds to a linear regression of the first half of the points of a, showing that a larger n_M the dephasing slows down slightly (due to relaxation of the water magnetization). When a bipolar gradient pair is inserted to bracket the DIPSI-2 mixing sequence (black crosses) the effect of RD on the DSS resonance is almost undistinguishable from the same experiment that does not use gradients for coherence pathway selection.

In figure 5 (left), the three components of the magnetization of the DSS methyl groups, recorded under the same conditions as figure 4 (curve a), are plotted as a function of n_M. Figure 6 (left) shows the result of an identical experiment, except that

https://doi.org/10.5194/mr-2021-65
Preprint. Discussion started: 6 December 2021

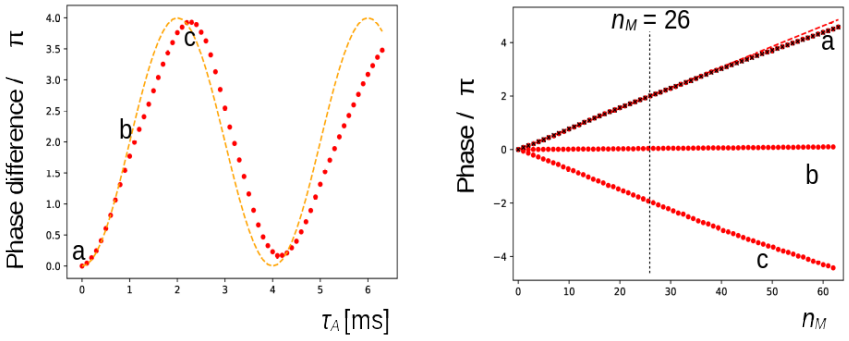

Figure 4. (left) The phase evolution of the methyl signal of DSS extracted from the experiment shown on the right side of figure 3 ($n_M = 26$). The duration of the preparatory pulse applied on H_2O varied from 0 to 6.3 ms with increments of 0.1 ms (maximum nutation angle of $ca.$ 3π). The orange dashed line shows the expected variation for an ideal RF pulse. (right) At positions a (0 ms), b (1.1 ms, complete saturation) and c (2.2 ms, inversion) the phase evolution of the signal is shown for $0 < n_M < 63$ with increments of 1. The red dashed line corresponds to a linear fit of the first 32 points of a. The black crosses are recorded under the same conditions of a after inserting a bipolar gradient pair before and after the mixing period as explained in figure 2.

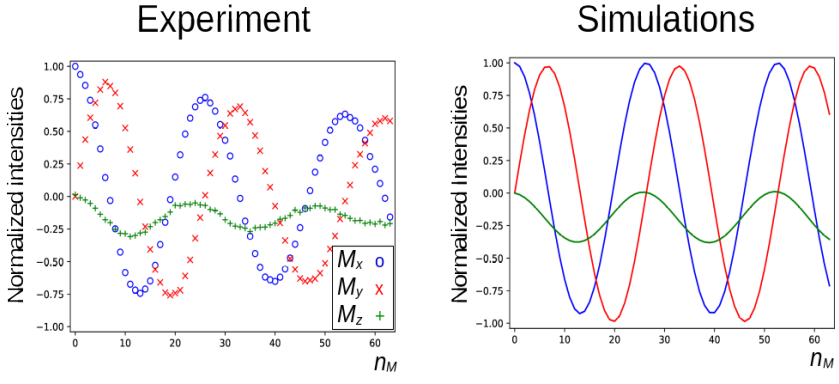

Figure 5. Evolution of the magnetization of the methyl resonance of DSS under the experimental conditions of figure 4 (curve a). For the calculations on the right the RD rate was estimated to be $R_R = 33.4 \times 2\pi$ Hz and $\psi = 29.8°$.

the carrier frequency has been moved to the solvent resonance, and that the amplitude of the selective Gaussian pulse has been increased in order to overcome RD effects during this pulse, so that the solvent magnetization is rotated in the xy-plane. Here, the z-component of the magnetization must be detected without changing the phase of the receiver for the different scans. Without RD, the magnetization of the methyl groups is expected to stay along the z-axis. Clearly, effects of the RD field are also observed in the latter experiment.

https://doi.org/10.5194/mr-2021-65
Preprint. Discussion started: 6 December 2021

Open Access MAGNETIC RESONANCE Discussions

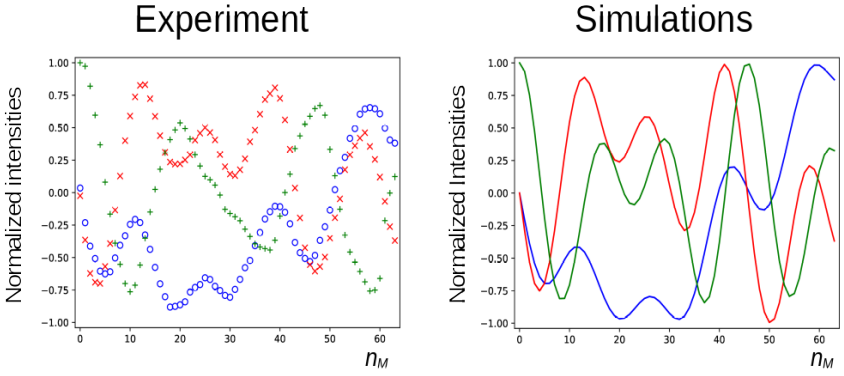

Figure 6. Same as figure 5, with the carrier frequency set on H_20 (conditions before mixing as in figure 2e), the same symbols as in figure 5 correspond to the same components of the magnetization. The RD parameters for the simulations on the right were the same as in figure 5.

4 Theory and Discussion

In order to explain the experimental results, the homo-nuclear case of abundant spins A (H_2O), whose magnetization induces an RD field in the coil as shown in figure 1, and sparse spins S (the three methyl groups in DSS), whose RD interaction with the coil can be neglected, will be considered. In the rotating frame, the evolution of the two (uncoupled) types of spins can be described by the modified Bloch equations (Bloom (1957)):

$$\frac{dM_x^i(t)}{dt} = -\omega_0^i M_y^i(t) + \omega_{1y}(t) M_z^i(t) - \{c_{Rx}(t) - s_{Ry}(t)\} M_z^i(t), \tag{1}$$

$$\frac{dM_y^i(t)}{dt} = \omega_0^i M_x^i(t) - \omega_{1x}(t) M_z^i(t) - \{c_{Ry}(t) + s_{Rx}(t)\} M_z^i(t), \tag{2}$$

$$\begin{aligned}\frac{dM_z^i(t)}{dt} = &- \omega_{1y}(t) M_x^i(t) + \omega_{1x}(t) M_y^i(t) \\ &+ \{c_{Rx}(t) - s_{Ry}(t)\} M_x^i(t) + \{c_{Ry}(t) + s_{Rx}(t)\} M_y^i(t),\end{aligned} \tag{3}$$

with i either spin A or S, ω_0^i the difference between the resonance frequency of spin i and the carrier frequency, ω_{1x} and ω_{1y} the x and y components of the RF field during the mixing sequence, while the remaining terms in the equations are due to the RD field:

$$\begin{aligned}&c_{Rx}(t) = \alpha_R M_x^A(t)\cos(\psi),\ s_{Rx}(t) = \alpha_R M_x^A(t)\sin(\psi), \\ &c_{Ry}(t) = \alpha_R M_y^A(t)\cos(\psi),\ s_{Ry}(t) = \alpha_R M_y^A(t)\sin(\psi),\end{aligned} \tag{4}$$

where the amplitude of the RD field is $\omega_R(t) = \alpha_R \sqrt{M_x^A(t)^2 + M_y^A(t)^2}$ and its phase is given by the angle ψ as indicated in figure 1. The proportionality constant α_R depends on the characteristics of the RF circuit:

$$\alpha_R = \mu_0 \eta \gamma Q/2\,, \tag{5}$$

https://doi.org/10.5194/mr-2021-65
Preprint. Discussion started: 6 December 2021


Open Access MAGNETIC RESONANCE Discussions

with μ_0 the vacuum permeability, γ the gyro-magnetic ratio of the protons, η the filling factor of the sample and Q the quality factor of the RF circuit. By a multiplication of α_R with the equilibrium magnetization of the abundant spins A, the use of the RD rate

$$R_R = \alpha_R M_{eq}^A \,, \tag{6}$$

allows one to use normalized magnetization vectors ($i.e.$, divide all components of spin i by M_{eq}^i) in equations 1-4.

The evolution of the magnetization of both A and S nuclei during the TOCSY pulse train has been numerically simulated using the above equations. First the evolution of $\boldsymbol{M}^A(t)$ was determined. For spin S equations 1-3 reduce to the traditional Bloch equations, with the magnetization of spin A as a source of a time-dependent RF field. The values of the rate R_R and the angle ψ were estimated to give a qualitative agreement with the data, as shown in figure 5, rather than an exact fit. The combination of the two parameters is not unique, a smaller angle ψ can be compensated by a larger value of R_R. The use of the RD parameters extracted from the signal of H_20 after a simple pulse-acquire experiment does not lead to a good agreement. This is likely due to the fact that the RF circuit is not the same during signal acquisition as during the application of RF pulses (Marion and Desvaux (2008)). In figure 5, the agreement between simulations and experiments is quite satisfactory. The decay of the experimental curves is not only due to relaxation but also to RF inhomogeneities: the precession frequency of the DSS signal varies slightly with the the RF amplitude, while the evolution of the z component is even more sensitive (simulations not shown).

For the curves on the right-hand side of figure 6 the same RD parameters in figure 5 have been used. In the simulations, the fact that, due to RD effects, the water magnetization is not aligned along the x-axis after the first $\pi/2$ pulse has been taken into account (a phase shift of -18° was determined experimentally). The agreement between experiments and simulations is adequate, considering the fact that neither RF inhomogeneity and calibration errors nor relaxation effects have been taken into account. Moreover, the evolution is very sensitive to the exact position of the water magnetization after the selective Gaussian pulse.

The phenomenon shown in this work strongly depends on the characteristics of the probe. Similar results (not shown), albeit much smaller in magnitude, have been obtained at 18.8 T (800 MHz proton frequency) on a traditional “room temperature” probe.

5 Conclusions

It has been shown RD can strongly perturb the evolution of magnetization of spins that are neither directly coupled by scalar or dipolar interactions to the source spins nor have a nearby resonance frequency. Counter-intuitively, the RD field can thus cause the magnetization of remote resonances to precess notwithstanding the presence of a much stronger RF spin-locking pulse-train. This effect increases with increasing RF amplitudes (results not shown). It can be prevented by saturating or dephasing the magnetization of the spins that cause radiation damping.

https://doi.org/10.5194/mr-2021-65
Preprint. Discussion started: 6 December 2021


Open Access MAGNETIC RESONANCE Discussions

120 *Author contributions.* $N.A$

Competing interests. The author has no conflicts of interest to declare.

Acknowledgements. I thank Vineeth Francis Thalakottoor for help with the simulations and Geoffrey Bodenhausen for correcting the manuscript.

https://doi.org/10.5194/mr-2021-65
Preprint. Discussion started: 6 December 2021

Open Access MAGNETIC RESONANCE Discussions

References

Abragam, A.: The principles of nuclear magnetism., Clarendon Press, Oxford, 1961.

Bax, A. and Davis, D.: Mlev-17-Based Two-Dimensional Homonuclear Magnetization Transfer Spectroscopy, J. Magn. Reson., 65, 355–360, https://doi.org/10.1016/0022-2364(85)90018-6, 1985.

Bloembergen, N. and Pound, R.: Radiation Damping in Magnetic Resonance Experiments, Phys. Rev., 95, 8–12, https://doi.org/10.1103/PhysRev.95.8, 1954.

Bloom, S.: Effects of Radiation Damping on Spin Dynamics, J. Appl. Phys., 28, 800–805, https://doi.org/10.1063/1.1722859, 1957.

Braunschweiler, L. and Ernst, R.: Coherence Transfer by Isotropic Mixing - Application to Proton Correlation Spectroscopy, J. Magn. Reson., 53, 521–528, https://doi.org/10.1016/0022-2364(83)90226-3, 1983.

Broekaert, P. and Jeener, J.: Suppression of Radiation Damping in NMR in Liquids by Active Electronic Feedback, J. Magn. Reson. Ser. A, 113, 60–64, https://doi.org/10.1006/jmra.1995.1056, 1995.

Chen, J. H. and Mao, X. A.: Radiation damping transfer in nuclear magnetic resonance experiments via chemical exchange, J. Chem. Phys., 107, 7120–7126, https://doi.org/10.1063/1.474953, 1997.

Dalvit, C. and Bovermann, G.: Pulsed-Field Gradient One-Dimensional Nmr Selective Roe and Tocsy Experiments, Magn. Reson. Chem., 33, 156–159, https://doi.org/10.1002/mrc.1260330214, 1995.

Davis, D. and Bax, A.: Simplification of H-1-Nmr Spectra by Selective Excitation of Experimental Subspectra, J. Am. Chem. Soc., 107, 7197–7198, https://doi.org/10.1021/ja00310a085, 1985.

Hobson, R. and Kaiser, R.: Some Effects of Radiation Feedback in High-Resolution Nmr, J. Magn. Reson., 20, 458–474, https://doi.org/10.1016/0022-2364(75)90003-7, 1975.

Hoult, D. I. and Bhakar, B.: NMR signal reception: Virtual photons and coherent spontaneous emission, Concepts Magn. Reson., 9, 277–297, https://doi.org/10.1002/(SICI)1099-0534(1997)9:5<277::AID-CMR1>3.0.CO;2-W, 1997.

Kessler, H., Oschkinat, H., Griesinger, C., and Bermel, W.: Transformation of Homonuclear Two-Dimensional Nmr Techniques into One-Dimensional Techniques Using Gaussian Pulses, J. Magn. Reson., 70, 106–133, https://doi.org/10.1016/0022-2364(86)90366-5, 1986.

Krishnan, V. V. and Murali, N.: Radiation damping in modern NMR experiments: Progress and challenges, Prog. Nucl. Magn. Reson. Spectrosc., 68, 41–57, https://doi.org/10.1016/j.pnmrs.2012.06.001, 2013.

Louisjoseph, A., Abergel, D., and Lallemand, J.: Neutralization of Radiation Damping by Selective Feedback on a 400-Mhz Nmr Spectrometer, J. Biomol. NMR, 5, 212–216, 1995.

Marion, D. J.-Y. and Desvaux, H.: An alternative tuning approach to enhance NMR signals, J. Magn. Reson., 193, 153–157, https://doi.org/10.1016/j.jmr.2008.04.026, 2008.

Miao, X. J., Chen, J. H., and Mao, X. A.: Selective excitation by radiation damping field for a coupled nuclear spin system, Chem. Phys. Lett., 304, 45–50, https://doi.org/10.1016/S0009-2614(99)00291-2, 1999.

Rucker, S. and Shaka, A.: Broad-Band Homonuclear Cross Polarization in 2d Nmr Using Dipsi-2, Mol. Phys., 68, 509–517, https://doi.org/10.1080/00268978900102331, 1989.

Shampine, L.: Some Practical Runge-Kutta Formulas, Math. Comput., 46, 135–150, https://doi.org/10.2307/2008219, 1986.

Sobol, A. G., Wider, G., Iwai, H., and Wuthrich, K.: Solvent magnetization artifacts in high-field NMR studies of macromolecular hydration, J. Magn. Reson., 130, 262–271, https://doi.org/10.1006/jmre.1997.1287, 1998.

Suryan, G.: Nuclear Magnetic Resonance and the Effect of the Methods of Observation, Curr. Sci., 18, 203–204, 1949.

https://doi.org/10.5194/mr-2021-65
Preprint. Discussion started: 6 December 2021

Szoke, A. and Meiboom, S.: Radiation Damping in Nuclear Magnetic Resonance, Phys. Rev., 113, 585–586, https://doi.org/10.1103/PhysRev.113.585, 1959.

Virtanen, P., Gommers, R., Oliphant, T. E., Haberland, M., Reddy, T., Cournapeau, D., Burovski, E., Peterson, P., Weckesser, W., Bright, J., van der Walt, S. J., Brett, M., Wilson, J., Millman, K. J., Mayorov, N., Nelson, A. R. J., Jones, E., Kern, R., Larson, E., Carey, C. J., Polat, I., Feng, Y., Moore, E. W., VanderPlas, J., Laxalde, D., Perktold, J., Cimrman, R., Henriksen, I., Quintero, E. A., Harris, C. R., Archibald, A. M., Ribeiro, A. H., Pedregosa, F., and van Mulbregt, P.: SciPy 1.0: fundamental algorithms for scientific computing in Python, Nat. Methods, 17, 261–272, https://doi.org/10.1038/s41592-019-0686-2, 2020.

Vlassenbroek, A., Jeener, J., and Broekaert, P.: Radiation Damping in High-Resolution Liquid Nmr - a Simulation Study, J. Chem. Phys., 103, 5886–5897, https://doi.org/10.1063/1.470468, 1995.